MNRAS **000**, 1–6 (2017) Preprint 20 April 2017 Compiled using MNRAS LATEX style file v3.0

Understanding Redshift-Space Distortions: How the Pairs Move

Joseph Kuruvilla[1]★† and Cristiano Porciani[1]
[1]*Argelander-Institut für Astronomie, University of Bonn, Auf dem Hügel 71, D-53121 Bonn, Germany*

Accepted XXX. Received YYY; in original form ZZZ

ABSTRACT
Streaming model ... More abstract

Key words: keyword1 – keyword2 – keyword3

1 INTRODUCTION

Redshift-space distortions – growth rate – Aim of the paper – Section 2 – Section 3

2 N-BODY SIMULATIONS

3 STREAMING EQUATION

Peculiar velocity distorts the true isotropic spatial distribution. Anisotropy in the spatial distribution introduced by the line-of-sight component of the peculiar velocity can be quantified in the configuration space by the 2-point correlation function. Fig 1 shows the isotropic nature of the correlation function in the real-space and the anisotropy introduced by the peculiar velocity in the redshift-space. The interesting objective now is knowing the real-space isotropic correlation function, how can we obtain the anisotropic redshift-space correlation function. One of the ways to model this is to use the streaming equation.

The streaming equation (Peebles 1993; Fisher 1995; Scoccimarro 2004) quantifies the anisotropic correlation function as a convolution of the true isotropic correlation function with the distribution of relative line-of-sight velocities. In the context of the distant observer approximation, it is written as

$$1+\xi_s(s_\parallel,s_\perp)=\int_{-\infty}^{\infty}\left[1+\xi_{\rm R}(r)\right]P_{v_{\rm los}}\left(s_\parallel-r_\parallel\mid r_\parallel,r_\perp\right){\rm d}r_\parallel\,, \quad (1)$$

where $r=\sqrt{r_\parallel^2+r_\perp^2}$ and $v_{\rm los}$ is the relative line-of-sight velocity. We set the line-of-sight axis along the z-axis for the remainder of this paper. The pair weighted quantity, $v_{\rm los}$, can then be defined as

$$v_{\rm los}=(\mathbf{v}_2-\mathbf{v}_1)\cdot\hat{\mathbf{r}}_{\rm los}=v_\parallel{\rm sgn}\left(r_\parallel\right), \quad (2)$$

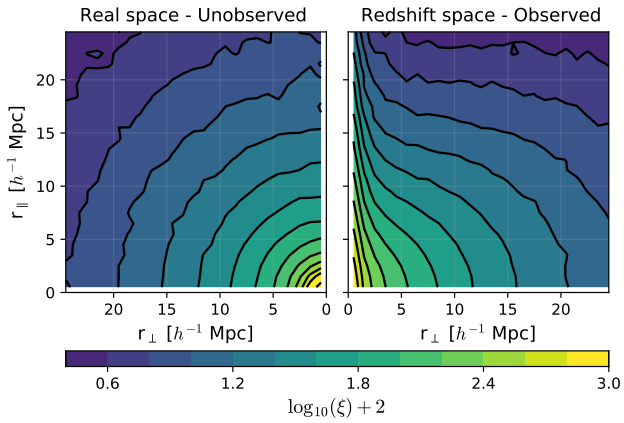

Figure 1. Correlation function in real-space and redshift-space.

where

$$v_\parallel=v_{z_2}-v_{z_1}\,, \quad (3)$$
$$r_\parallel=r_{z_2}-r_{z_1}\,. \quad (4)$$

3.1 Ingredients

In this section, we discuss about the three ingredients (i.e. the 2D anisotropic redshift-space correlation function, 1D isotropic real-space correlation function and the relative line-of-sight velocity distribution) entering the streaming equation. Firstly we turn our focus to the 1D real-space correlation function $\xi_R(r)$. The correlation functions were computed using the Landy-Szalay (LS) estimator (Landy & Szalay 1993), which is

$$\xi(r)=\frac{DD(r)-2DR(r)+RR(r)}{RR(r)}, \quad (5)$$

where $DD(r)$ is the normalised count of galaxy pairs, $DR(r)$ gives the normalised count of pairs given a cross correlation

★ E-mail: joseph.k@uni-bonn.de
† Member of the International Max Planck Research School (IMPRS) for Astronomy and Astrophysics at the Universities of Bonn and Cologne

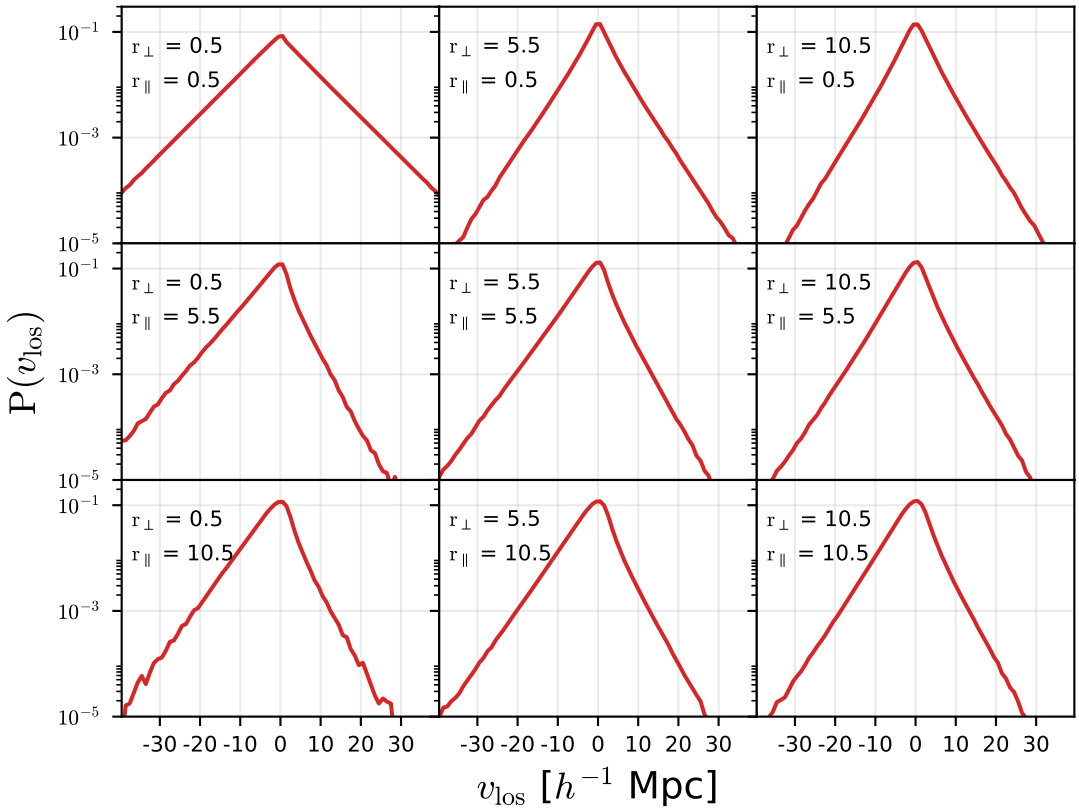

Figure 2. Relative line-of-sight velocity distribution. The distance mentioned in each subplot refers to the mean value of each bin, having a bin width of 1 h^{-1} Mpc.

between pairs and random points drawn from a random distribution and $RR(r)$ is the normalised count of random pairs. In order to mimic the redshift-space distortion effect in the simulation, we displace the position of the particles according to

$$\mathbf{s} = \mathbf{x} + \frac{v_z}{aH(a)}\hat{\mathbf{z}}, \tag{6}$$

where a is the scale factor and $H(a)$ is the Hubble factor. The "true" 2D redshift-space correlation function is then computed again using LS estimator on these displaced particles.

The relative line-of-sight velocity was measured using Eq. 2. For this purpose, we developed a Cython code[1] which is fully parallelised using MPI. The distribution was calculated from randomly down sampled selection of 256^3 particles. The total number of pairs we obtained from this sample is 5.1×10^{11} at distances from 0.5 to 100.5 h^{-1} Mpc between the pairs. For the completeness, we have included the periodic boundary conditions while measuring the distance between the pairs. The convergence property of the distribution has been tested with a higher particle number and discussed further in App. A. We showcase the relative line-of-sight velocity distribution computed for 256^3 particles in Fig. 2. One of the immediate conclusion we can draw upon visual inspection is that the distribution changes starkly with the distance and neither an exponential nor a Gaussian will be able to model the distribution accurately.

To further understand the distribution we try to characterise the distribution using moments. We specifically look into the the first raw moment (mean), the second central moment (variance), the third and the fourth standardised moments (skewness and kurtosis). Fig. 3 shows these moments of the relative line-of-sight velocity distribution.. The distribution is marked by non-zero skewness, specifically it is negatively skewed at all the scales shown. Due to the negative skewness, it can be seen that the mean velocity is negative at most scales. We can interpret this as it is more probable to have in-falling pairs at these scales (Scoccimarro 2004). The distribution showcases a leptokurtic behaviour, implying it has a fatter tail than a normal distribution which has a skewness value of 3.

Having all the ingredients needed, we compute the integral of the streaming equation (Eq. 1) and compare it with the "true" redshift-space correlation function measured from the simulations. This is shown in Fig. 4. It seems that when one checks Eq. 1 with simulations there seems to be some discrepancy even though it has been quoted to be exact. The deviation from exactness is worrying as all the phenomenological streaming models are build upon the streaming equation. To understand the discrepancy, we go back to the roots from which we derived the streaming in the next section and try to understand why this deviation from exactness arises.

[1] https://github.com/jkuruvilla

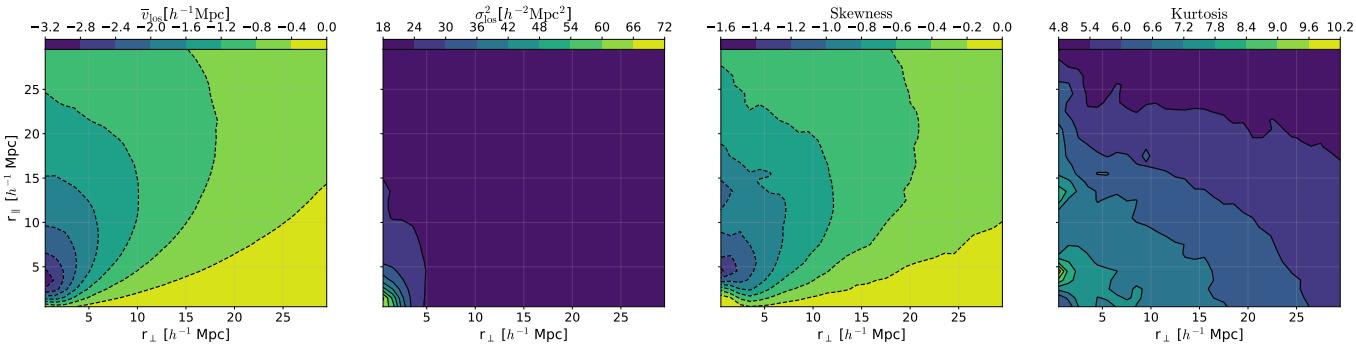

Figure 3. Characterising the relative line-of-sight velocity distribution. First panel on left shows the mean relative velocity, followed by the velocity dispersion. The third and the fourth panels shows the standardised moments skewness and kurtosis respectively. Skewness is a measure of the symmetry of the distribution while kurtosis acts as a measure of the tailedness of the distribution

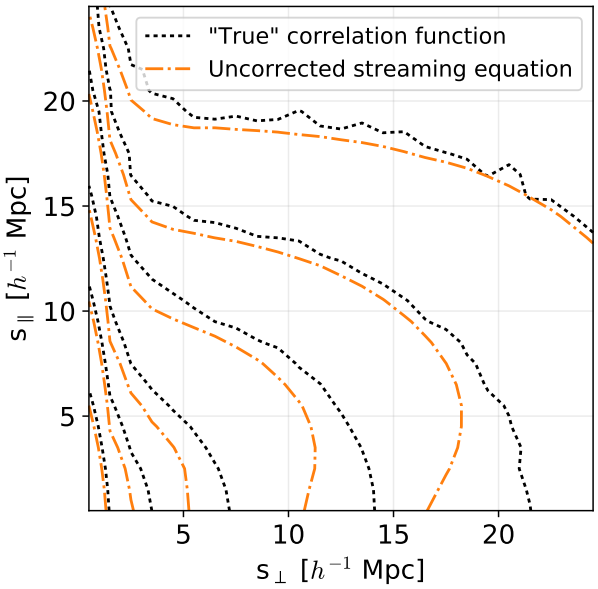

Figure 4. Uncorrected

4 CORRECTIONS TO STREAMING EQUATION

Correlation function in redshift space can be defined as the probability to find a pair at parallel and perpendicular to line-of-sight distance ($s_\parallel$ and $s_\perp$), which is given as

$$\mathrm{d}P = 2\pi s_\perp n \left[1 + \xi_s(s_\parallel, s_\perp)\right] \mathrm{d}s_\parallel \, \mathrm{d}s_\perp \,, \tag{7}$$

where $\xi_s(s_\parallel, s_\perp)$ is the 2D anisotropic redshift-space correlation function. This could also written in terms of real space quantities as

$$\mathrm{d}P = 2\pi s_\perp n \left[1 + \xi_{\mathrm{R}}(r)\right] P_{v_{\mathrm{los}}}\left(v_{\mathrm{los}} \mid r_\parallel, r_\perp\right) \delta_{\mathrm{D}}\left(\left(s_\parallel - r_\parallel\right) \mathrm{sgn}\left(r_\parallel\right) - v_{\mathrm{los}}\right) \mathrm{d}r_\parallel \, \mathrm{d}s_\parallel \, \mathrm{d}s_\perp \, \mathrm{d}v_{\mathrm{los}} \,. \tag{8}$$

where $\xi_{\mathrm{R}}(r)$ is the isotropic real-space correlation function and $P_{v_{\mathrm{los}}}\left(v_{\mathrm{los}} \mid r_\parallel, r_\perp\right)$ is the relative line-of-sight velocity distribution function. The term inside the Dirac-delta ensures $s_\parallel = r_\parallel + v_\parallel$, which shows how the pairs are displaced.

Comparing Equations (7) and (8), and integrating over v_{los} and $r_\parallel$ eliminates the delta function, one obtains

$$1 + \xi_s(s_\parallel, s_\perp) = \int_{-\infty}^{\infty} \left[1 + \xi_{\mathrm{R}}(r)\right] P_{v_{\mathrm{los}}}\left(\left(s_\parallel - r_\parallel\right) \mathrm{sgn}\left(r_\parallel\right) \mid r_\parallel, r_\perp\right) \mathrm{d}r_\parallel \,. \tag{9}$$

This is the streaming equation, which is exact in the distant-observer approximation. It is to be noted that Eq. 9 is different to the usual streaming equation as seen in literature till now. We can then proceed to break the integral in the following manner

$$1 + \xi_s(s_\parallel, s_\perp) = \int_{-\infty}^{0} \left[1 + \xi_{\mathrm{R}}(r)\right] P_{v_{\mathrm{los}}}\left(r_\parallel - s_\parallel \mid r_\parallel, r_\perp\right) \mathrm{d}r_\parallel + \int_{0}^{\infty} \left[1 + \xi_{\mathrm{R}}(r)\right] P_{v_{\mathrm{los}}}\left(s_\parallel - r_\parallel \mid r_\parallel, r_\perp\right) \mathrm{d}r_\parallel \,. \tag{10}$$

Fig. 5 shows the corrected streaming equation (Eq. 10) compared with the simulation. One can clearly see that with the complete knowledge of the relative line-of-sight velocity distribution and with the correction to account for the pairs which have flipped, we are able to reproduce the true redshift space correlation function accurately.

It is interesting to note that the integral runs from -∞ to +∞. So what does the negative $r_\parallel$ mean in the context of streaming model? It means that if we are to take the redshift space to be our reference frame, the negative $r_\parallel$ implies pairs which have flipped their position compared to their redshift space counterparts. Fig. 8 clearly demonstrates this where the negative $r_\parallel$ is the distance between the pairs which have flipped their position in real-space as compared to the position in redshift-space. It should be noted again that the redshift-space distortions is purely a line-of-sight effect, hence the perpendicular distance between the pairs remains unchanged.

4.1 Can we use pairwise velocity?

The relative line-of-sight velocity can be related to the radial and tangential pairwise velocity as follows

$$v_{\mathrm{los}} = \mathrm{sgn}(r_\parallel) \left[v_{\mathrm{r}} \cos\theta + v_{\mathrm{T}} \sin\theta\right] \,, \tag{11}$$

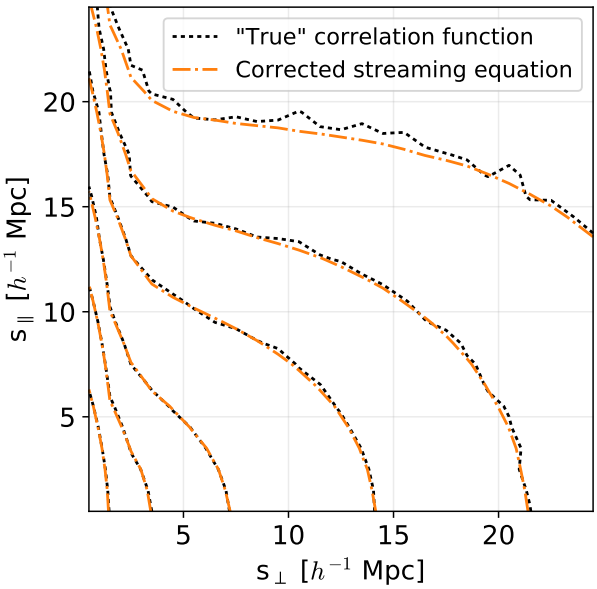

Figure 5. Corrected streaming equation compared with the simulation. Orange line denotes the correlation function obtained using the corrected streaming equation(Eq. 10) and black dashed line denotes to the redshift space correlation function measured directly from simulation.

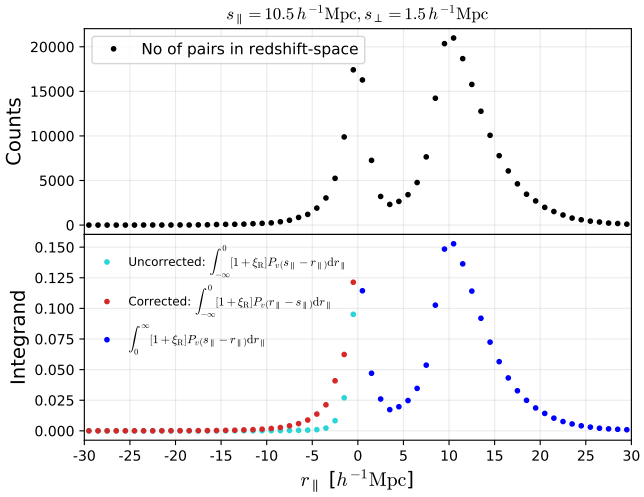

Figure 6. Consistency check for the streaming equation. Top panel: Shows the number of pairs in redshift-space for particular $s_\parallel$ and $s_\perp$. $r_\parallel$ is obtained as $s_\parallel - v_\parallel$. Bottom panel: Shows the integrand distribution of the streaming equations at same $s_\parallel$ and $s_\perp$ as top panel. Due to using the wrong argument of the PDF in the uncorrected integrand, the final value will be undermined compared to the true value.

where v_r and v_T are the radial and tangential components of the pairwise velocity respectively. They are defined as

$$v_r = (\mathbf{v}_2 - \mathbf{v}_1)\cdot\hat{\mathbf{r}}, \tag{12}$$

$$v_T = \mathrm{sgn}(v_{t_z})\,|\mathbf{v}_t|, \tag{13}$$

$$\mathbf{v}_t = (\mathbf{v}_2 - \mathbf{v}_1) - (v_r\cdot\hat{\mathbf{r}}) - (v_{away}\cdot\hat{\mathbf{n}}_{12}), \tag{14}$$

$$v_{away} = (\mathbf{v}_2 - \mathbf{v}_1)\cdot\hat{\mathbf{n}}_{12}, \tag{15}$$

$$\mathbf{n}_{12} = (\mathbf{r}_2 - \mathbf{r}_1)\times\hat{\mathbf{z}}. \tag{16}$$

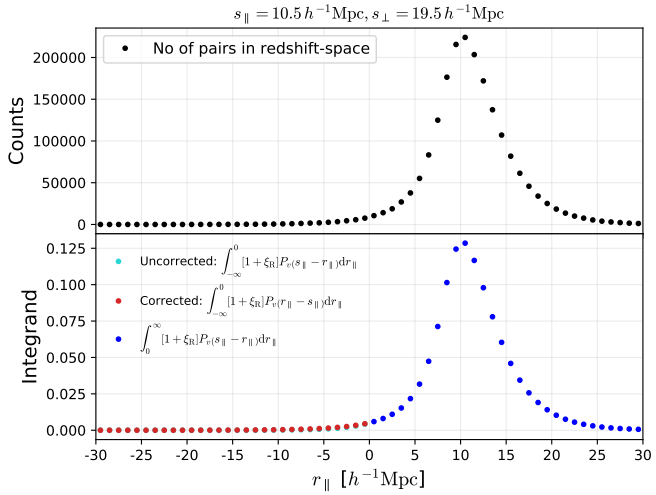

Figure 7. Same as Fig. 6, but for larger scales. Both the uncorrected (Eq. 1) and corrected (Eq. 10) streaming equations are equivalent at these scales. The impact of pair flips are negligible.

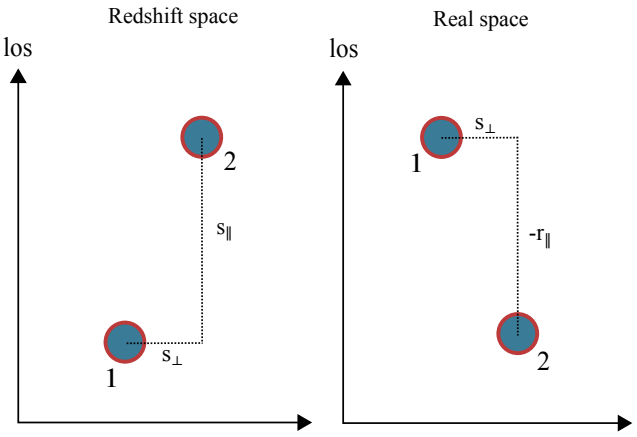

Figure 8. Flipped pairs

On averaging Eq. 11, we see that

$$\langle v_{los}\rangle = \mathrm{sgn}(r_\parallel)\left[\langle v_r\rangle\cos\theta + \langle v_T\rangle\sin\theta\right]. \tag{17}$$

However due to isotropy, $\langle v_T\rangle = 0$. Mean of the relative line-of-sight velocity is then

$$\langle v_{los}\rangle = \mathrm{sgn}(r_\parallel)\left[\langle v_r\rangle\cos\theta\right]. \tag{18}$$

$$\left\langle v_{los}^2\right\rangle = \left\langle v_r^2\right\rangle\cos^2\theta + \left\langle v_T^2\right\rangle\sin^2\theta, \tag{19}$$

$$\left\langle v_{los}^2\right\rangle = \left\langle v_r^2\right\rangle\cos^2\theta + \left\langle v_T^2\right\rangle\sin^2\theta, \tag{20}$$

where we have used $\langle v_r v_T\rangle = 0$. This has indeed been checked from the simulation and assured that this holds. In fact any term involving averaging of odd power of v_T disappears due to the isotropy. The second cumulant is then given as

$$\sigma_{los}^2 = \left\langle v_{los}^2\right\rangle - \langle v_{los}\rangle^2 \tag{21}$$

$$= \sigma_r^2\cos^2\theta + \sigma_T^2\sin^2\theta \tag{22}$$

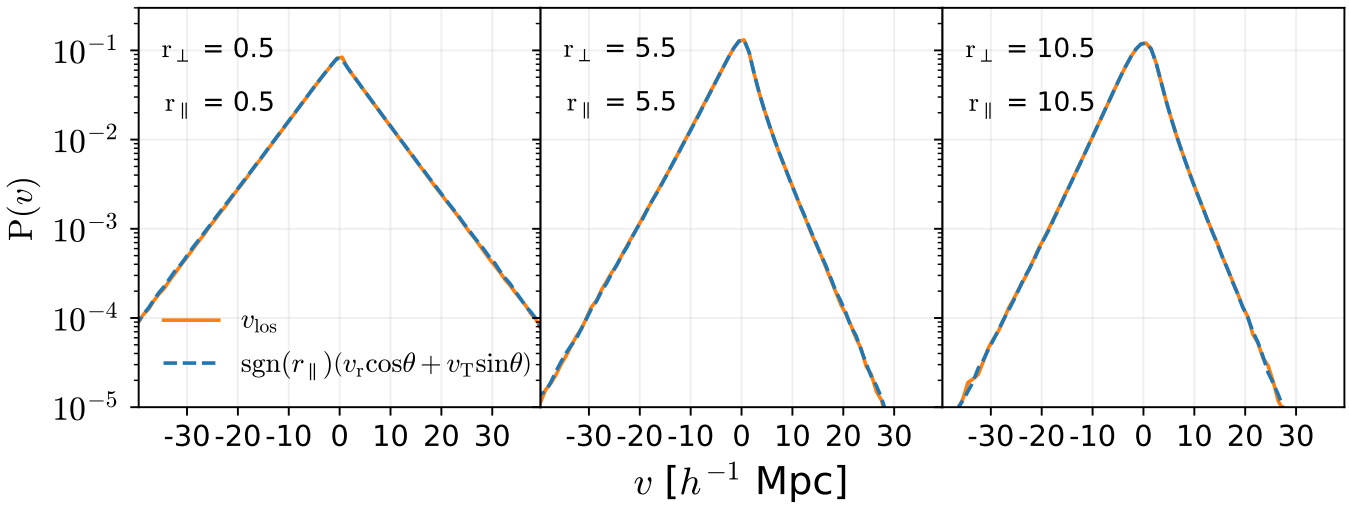

Figure 9. Shows the equivalence of relative line-of-sight velocity to the radial and the tangential component of the pairwise velocity as given by Eq. 11.

where $\sigma_r^2 = \left\langle v_r^2 \right\rangle - \langle v_r \rangle^2$ and $\sigma_T^2 = \left\langle v_T^2 \right\rangle$.

$$\left\langle v_{los}^3 \right\rangle = \left\langle v_r^3 \right\rangle \cos^3\theta + 3 \left\langle v_r v_T^2 \right\rangle \cos\theta \sin^2\theta, \tag{23}$$

The third cumulant of the relative line-of-sight velocity is defined as

$$\gamma_{los} = \left\langle v_{los}^3 \right\rangle - 3 \left\langle v_{los}^2 \right\rangle \langle v_{los} \rangle + 2 \langle v_{los} \rangle^3 \tag{24}$$

Using Eqs. 18, 19 and 23, it can be rewritten as

$$\gamma_{los} = sgn(r_\parallel) \left(\cos^3\theta \left[\left\langle v_r^3 \right\rangle - 3 \left\langle v_r^2 \right\rangle \langle v_r \rangle + 2 \langle v_r \rangle^3 \right] + 3 \cos\theta \sin^2\theta \left[\left\langle v_r v_T^2 \right\rangle - \langle v_r \rangle \left\langle v_T^2 \right\rangle \right] \right) \tag{25}$$

$$\gamma_{los} = sgn(r_\parallel) \cos\theta \left(\cos^2\theta\, \gamma_r + 3 \sin^2\theta\, Cov \left[v_r, v_T^2 \right] \right) \tag{26}$$

Thus we see that the third cumulant of the relative line-of-sight velocity not only depends on the third cumulant of the radial component of the pairwise velocity but also covariance between the radial and square of the tangential component of the pairwise velocity.

5 PHENOMENOLOGICAL MODEL

GH is the mixture modelling consisting of normal distribution and Generalised Inverse Gaussian distribution. It is similar to modelling pairwise velocity as mixture of the normal and log-normal density (see tinker). GIG and log-normal are very similar. Try to connect them and see. Density weighted velocity, so would make sense to connect them. Could explain why we use it and why they could be the true distribution/

6 DISSECTING VELOCITY DISTRIBUTION

To model accurately model the relative line-of-sight velocity distribution, it is important to understand how each component plays a role in the distribution. For this purpose, we classify the dark matter particles as either 'halo' particles or 'field' particle. This was done with the help of ROCKSTAR halo finder. Particles which were identified to belong to the halos were subsequently classified as 'halo' particles and the rest as 'field' particles.

Fig 10 shows the result of how the components contribute to the total distribution. At the very small scales as seen in the case of mean distance of $r_\perp = r_\parallel = 0.5h^{-1}$ Mpc, the distribution is powered by the halo-halo particle pairs. This is not surprising as at these scales, we expect the pairs to be mostly in halos. As the pair separation increases however, the field-field component seems to be the dominant factor especially at the peaks of the distribution. The mean infalling velocity hence seems to be driven by the field-field particle pairs. The narrow wings of the field-field component suggests that the pairs are which does not belong to halos undergo coherent motion. The wings of the total distribution are contributed by both the halo-halo and the field-halo pairs. This clearly shows how the non-Gaussian nature of the relative line-of-sight velocity distribution for the full DM particles arises from the combined effect of the field and halo particles.

red

7 CONCLUSIONS

ACKNOWLEDGEMENTS

JK acknowledges the financial support from the Bonn-Cologne Graduate School (BCGS).

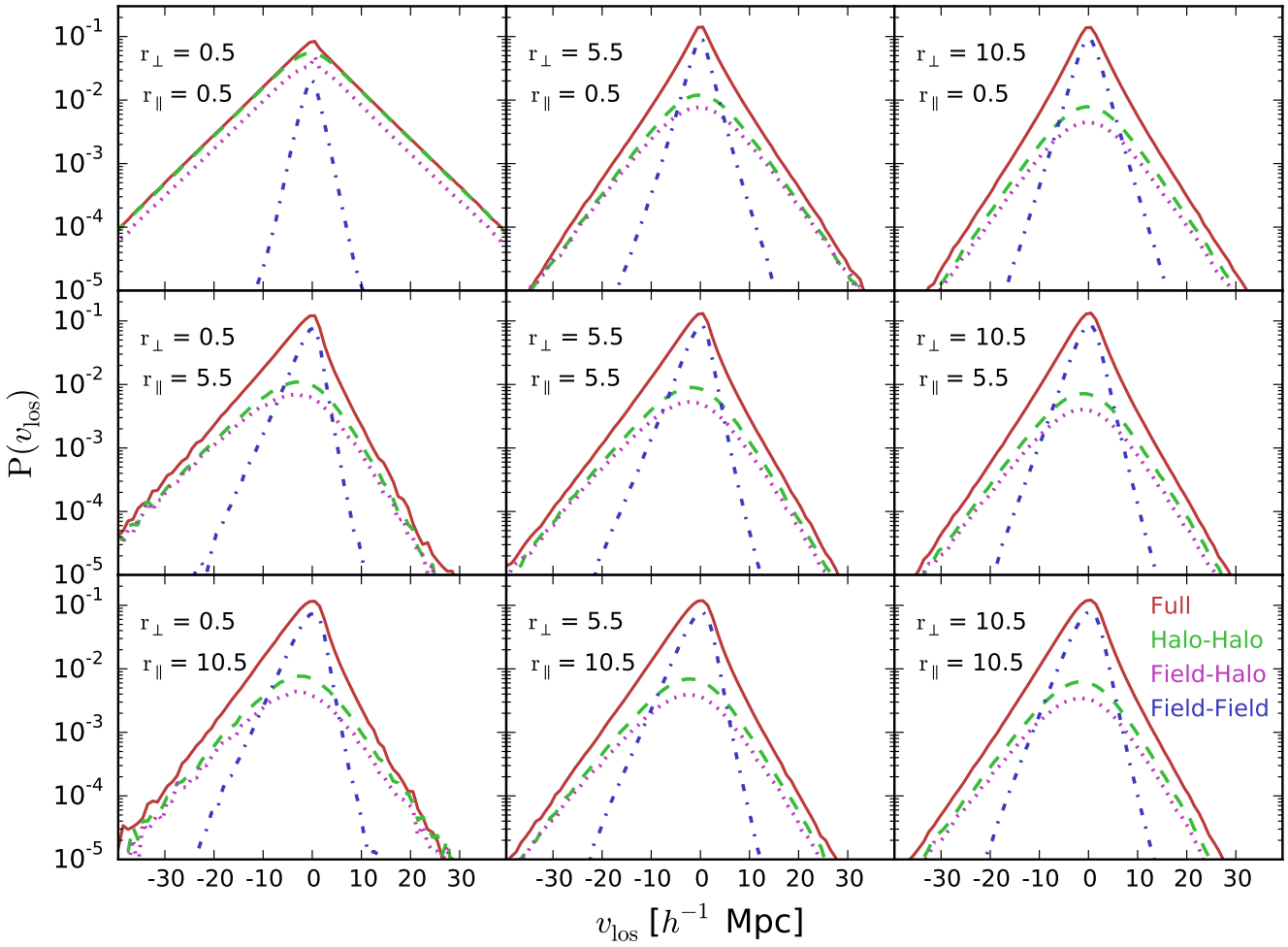

Figure 10. Relative line-of-sight velocity distribution for different components. Green dashed line refers to the pairs which are comprised of 2 halo particles, blue dash dotted line refers to the pair which are formed by 2 field particles and finally magenta dotted line showcases the distribution contributed by pairs in which one of the particle is a field particle and the other a halo particle. The distribution of the full particles is shown using the red solid line. The distance mentioned in each subplot refers to the mean value of each bin, having a bin width of 1 h^{-1} Mpc.

REFERENCES

Fisher K. B., 1995, ApJ, 448, 494
Landy S. D., Szalay A. S., 1993, ApJ, 412, 64
Peebles P. J. E., 1993, Principles of Physical Cosmology
Scoccimarro R., 2004, Phys. Rev. D, 70, 083007

APPENDIX A: CONVERGENCE

APPENDIX B: EXTRA

This paper has been typeset from a TEX/LATEX file prepared by the author.

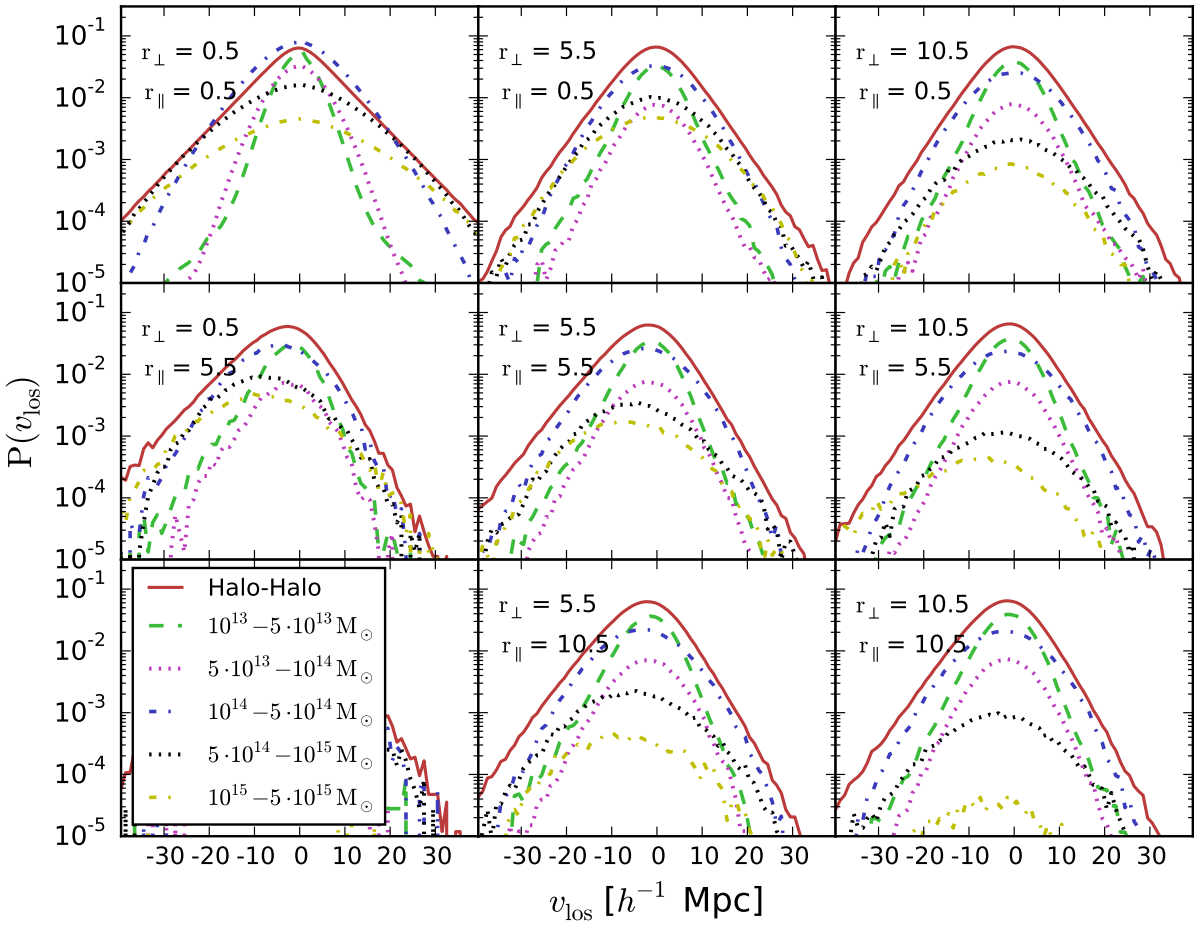

Figure 11. Relative line-of-sight velocity distribution for different components. Green dashed line refers to the pairs which are comprised of 2 halo particles, blue dash dotted line refers to the pair which are formed by 2 field particles and finally magenta dotted line showcases the distribution contributed by pairs in which one of the particle is a field particle and the other a halo particle. The distribution of the full particles is shown using the red solid line. The distance mentioned in each subplot refers to the mean value of each bin, having a bin width of 1 h^{-1} Mpc.

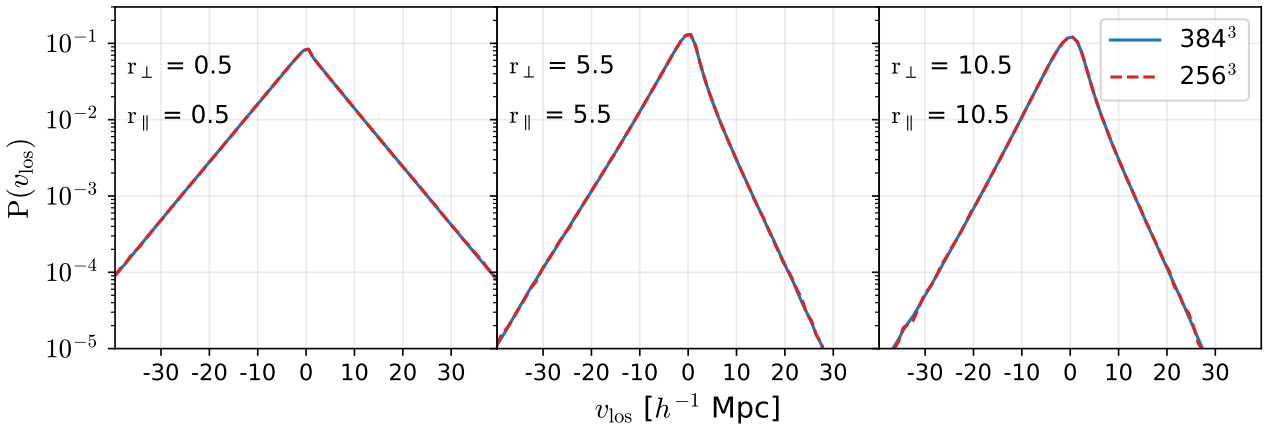

Figure A1. Relative line-of-sight velocity distribution. The distance mentioned in each subplot refers to the mean value of each bin, having a bin width of 1 h^{-1} Mpc.